Contents lists available at ScienceDirect

Applied Catalysis B: Environmental

Electrodeposited NiCu bimetal on carbon paper as stable non-noble anode for efficient electrooxidation of ammonia

Wei Xu [a,b], Dongwei Du [a], Rong Lan [a], John Humphreys [a], David N. Miller [c], Marc Walker [d], Zucheng Wu [b], John T.S. Irvine [c], Shanwen Tao [a,e,*]

[a] School of Engineering, University of Warwick, Coventry CV4 7AL, UK
[b] Department of Environmental Engineering, State Key Laboratory of Clean Energy Utilization, Zhejiang University, Hangzhou 310058, Zhejiang, China
[c] School of Chemistry, University of St Andrews, St Andrews, Fife KY16 9ST, UK
[d] Department of Physics, University of Warwick, Coventry CV4 7AL, UK
[e] Department of Chemical Engineering, Monash University, Clayton, Victoria 3800, Australia

ARTICLE INFO

ABSTRACT

Electrochemical remediation of ammonia-containing wastewater at low cell voltage is an energy-effective technology which can simultaneously recover energy via hydrogen evolution reaction. One of the main challenges is to identify a robust, highly active and inexpensive anode for ammonia electrooxidation. Here we present an alternative anode, prepared by electrochemical co-deposition of Ni and Cu onto carbon paper. This NiCu bimetallic catalyst is characterised by scanning electron microscope, scanning transmission electron microscope, X-ray diffraction, x-ray photoelelectron spectroscopy, cyclic voltammetry, linear sweep voltammetry and chronoamperometry techniques. The stability and activity of NiCu bimetallic catalyst are largely improved in comparison with Ni or Cu catalyst. Moreover this noble-metal-free NiCu catalyst even performs better than Pt/C catalyst, as NiCu is not poisoned by ammonia. An ammonia electrolysis cell is fabricated with NiCu/carbon paper as anode for ammonia electrolysis. The influences of pH value, applied cell voltages and initial ammonia concentration on cell current density, ammonia removal and energy efficiency are tested. An ammonia removal efficiency of ∼80% and coulombic efficiency up to ∼92% have been achieved. Ni-Cu bimetal on carbon paper is a stable non-noble anode for efficient electrooxidation of ammonia.

© 2016 The Authors. Published by Elsevier B.V. This is an open access article under the CC BY license (http://creativecommons.org/licenses/by/4.0/).

1. Introduction

The discharge of ammonia-containing wastewater into natural environment can damage ecological balance, which is known as eutrophication [1,2]. Normally biological methods are widely used for nitrogen removal in wastewater with the complex nitrification-denitrification processes [3,4]. The biochemical chain of nitrogen removal includes two steps, aerobic oxidation $NH_3 \rightarrow NO_2^- \rightarrow NO_3^-$ and anaerobic reduction $NO_3^- \rightarrow NO_2^- \rightarrow N_2$ [5]. Although biological treatment is a cost-saving way, it usually takes a long time. Besides, additional carbon source (e.g. methanol) is required when the carbon/nitrogen ratio of wastewater is low [6]. Many wastewater sources such as industry and landfill leachate are produced with a high value of ammonia concentration but a low value of C/N ratio [7,8], which limit the application of biological treatment.

Electrochemical treatment of ammonia has attracted more and more attention because it is easy-operation, environmental-friendly and applicable to tough conditions [9–12]. Ammonia can be directly converted to nitrogen gas at anode through a three-electron oxidation reaction [13–15].

Anode reaction : $NH_3(aq) + 3OH^- \rightarrow 1/2N_2O \uparrow + 3H_2O + 3e^-$

$$E_{anode} = -0.77\,V\,vs.SHE \tag{1}$$

Cathode reaction : $3H_2O + 3e^- \rightarrow 3/2H_2 \uparrow + 3OH^-$

$$E_{cathode} = -0.83\,V\,vs.SHE \tag{2}$$

Overall reaction : $NH_3(aq) \rightarrow 1/2N_2 \uparrow + 3H/2_2 \uparrow \Delta E = -0.06\,V \tag{3}$

* Corresponding author at: School of Engineering; University of Warwick, Coventry CV4 7AL, UK.
E-mail address: S.Tao.1@warwick.ac.uk (S. Tao).

Compared to biological method, electrooxidation of ammonia needs less step and simpler setup. Furthermore, hydrogen gas can be generated at cathode according to Reaction (2). In this way, the chemical energy in ammonia is retrieved in the form of hydrogen energy during ammonia electrolysis. The generated hydrogen can be utilized to produce power by combustion, fuel cells and hydrogen-forced engines, compensating for parts of the energy consumption in ammonia electrolysis [16–18].

Theoretically, only a small value of external energy (0.06 V) is required to crack ammonia to nitrogen and hydrogen [15]. It is much lower than the energy (1.23 V) required by water electrolysis:

$$\text{Water electrolysis}: 3H_2O \rightarrow 3H_2 \uparrow + 3/2O_2 \uparrow \Delta E^0_{H_2/H_2O} = 1.23V$$

(4)
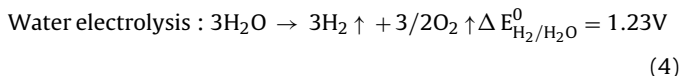
However, ammonia electrooxidation at anode is reported to be sluggish and have a large overpotential, thus it is important to develop high-performance electrocatalysts in order to solve this fundamental challenge [19]. Platinum and Pt-based catalysts are most active with small overpotential, but they are less affordable and easily poisoned by the adsorbed N_{ads}, and thus limiting the electrolysis current [20–22]. Transition metal Ni and Ni(OH)$_2$ based anode catalyst is a promising and inexpensive material for ammonia electrooxidation in alkaline condition [13,23]. Nevertheless they can be corroded and deactivate in ammonia solution resulting in a secondary pollution of metal ions [23,24]. Besides, copper also has high activity toward ammonia electrooxidation theoretically, which is comparable to Pt [22]. However it binds N atom too weakly so that it cannot catalytically oxidize ammonia experimentally.

One strategy to enhance activity and stability of metal catalyst is to incorporate another element into pure metal. Bimetallic NiCu catalyst is reported to have improved activity for methanol electrooxidation and water electrolysis [25–28], as well as enhanced stability [29]. In this work we present a method of electrodeposition of NiCu bimetal on carbon paper for ammonia electrooxidation. Carbon paper is used as supporting substrate for NiCu catalyst, because it has large surface area, high electric conductivity and chemical stability in alkaline ammonia electrolytes. NiCu coated carbon paper electrode is further used as noble-metal-free anode to fabricate ammonia electrolysis cell (AEC). This AEC can work under low cell voltage to achieve an energy-effective degradation, which is especially capable of ammonia-rich wastewater.

2. Experimental

2.1. Materials

Nickel(II) sulfate hexahydrate (NiSO$_4$·6H$_2$O, 98%, Alfa Aesar), and copper(II) sulfate pentahydrate (CuSO$_4$·5H$_2$O, 99.0%, Alfa Aesar) were utilized as metals precursors without any further purification. Carbon paper (28 mm, Toray 090, plain) was used as electrode substrate for electrodeposition. Nafion® solution (5 wt.%) were purchased from Sigma-Aldrich. Other chemicals like Pt/C (20 wt.%), NH$_4$Cl, KCl, K$_3$[Fe(CN)$_6$], sodium dodecyl sulfonate (SDS), isopropanol and NaOH were all analytical reagents and bought from Alfa Aesar.

2.2. Synthesis of NiCu bimetal on carbon paper

Carbon paper (2 cm²) was cleaned by HCl and ethanol first, and rinsed with deionized water as pre-treatment before electrodeposition. The NiCu/carbon paper (NiCu/CP) electrode was prepared by co-electrodepositing nickel and copper using potentiostatic technique. A solution composed of 0.5 M NiSO$_4$·6H$_2$O, 0.05 M CuSO$_4$·5H$_2$O and 0.5 M SDS was used as deposition electrolyte. The pre-treated carbon paper, Pt foil and Ag/AgCl functioned as working electrode, counter electrode and reference electrode, respectively. Deposition voltage was controlled at −1.3 V vs. Ag/AgCl for 20 s by an electrochemical interface (Solartron 1287A). Then the NiCu/CP was rinsed with deionized water and dried at 60 °C. The catalyst loading on CP was calculated by the weight difference of electrode after and before electrodeposition. For comparison, Ni/carbon paper and Cu/carbon paper electrodes were also prepared via similar method with the absence of CuSO$_4$·5H$_2$O or NiSO$_4$·6H$_2$O in the deposition electrolyte.

2.3. Catalyst characterization

The surface morphology of the as-obtained NiCu/CP electrode was studied by scanning electron microscope (SEM) (Zeiss SUPRA 55-VP) equipped with an energy-dispersive X-ray (EDX) spectrometer that allows elemental composition analysis. Compositional analysis was carried out using a FEI Titan Themis scanning transmission electron microscope (STEM) equipped with a Super-X windowless EDX detector system. Samples for STEM characterisation were prepared by dispersing specimen powder on a carbon film supported on a gold grid. The X-ray diffraction (XRD) patterns of NiCu/CP were recorded with Panalytical X-Pert Pro MPD with Cu K$_{\alpha 1}$ radiation. The x-ray photoelelectron spectroscopy (XPS) data were collected using an Omicron Multiprobe with the sample being illuminated using an XM1000 monchromatic Al kα x-ray source (Omicron Nanotechnology).

Electrochemical characterization of the NiCu/CP electrode was determined by cyclic voltammetry (CV), linear sweep voltammetry (LSV) and chronoamperometry (CA) techniques conducted by Solartron 1287A Electrochemical Interface in a three-electrode cell. A platinum foil and an Ag/AgCl electrode (saturated KCl) were used as the counter and reference electrode, respectively. The CV measurements, from 0.05 V to 0.7 V with a scan rate of 25 mV s^{-1}, were recorded after at least 5 cycles till stable results. The sweep rate of LSV is 1 mV s^{-1}. Electrochemical impedance spectroscopy (EIS) measurements were carried out by a Solartron 1287A/1250 in the frequency range of 60 kHz to 0.01 Hz at a bias 10 mV at an applied voltage of 0.55 V.

2.4. Fabrication of ammonia electrolysis cell and measurements

Carbon supported Pt (Pt/C) particles were dispersed in a mixture of Nafion® solution, isopropanol and deionized water under ultrasonic to get catalyst ink. Then it was brushed onto carbon paper (2 cm²) to prepare cathode of AEC for hydrogen evolution reaction. The Pt/C was also used as anode for comparison. The Pt loading on carbon paper was 0.3 mg cm^{-2}. NiCu/CP without any pre-activation was directly used as anode of AEC in a sealed glass cell containing 11 mL electrolyte. The initial ammonia concentration and pH of electrolyte was modified by NH$_4$Cl and 1 M NaOH. Ammonia electrolysis was studied under constant cell voltage in static batch model controlled by Solartron 1470E. Liquid samples were diluted and analysed by ammonia/pH meter equipped with ammonia ion selective electrode (Thermo Scientific Orion Star A214) to detect ammonia concentration at appropriate intervals. Nitrate, copper and nickel ions were detected by ion chromatography equipped with an electrical conductivity detector (Metrohm® 883 IC, with Metrosep C 4 − 250/4.0 column for cations and ICSep AN2 column for anions). The anodic coulombic efficiency (η_a) was based on NH$_3$ oxidized to N$_2$, and calculated according to the following equation:

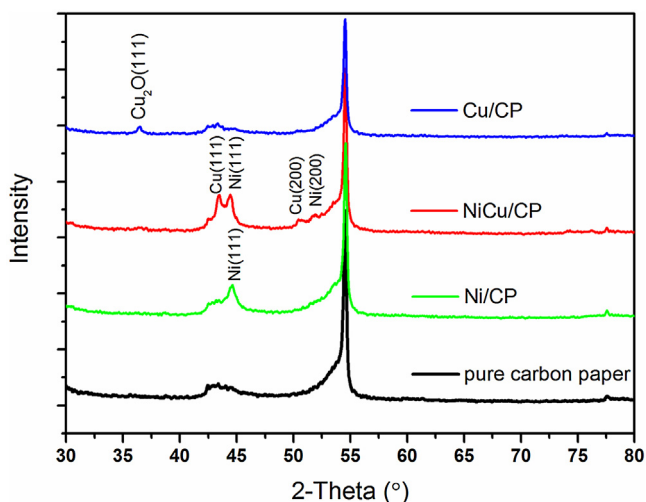$$\eta_a = \frac{Q_e}{Q_f} = \frac{nFV(C_0 - C_t)/17000}{\int Idt}$$

(5)

Fig. 1. X-ray diffraction patterns of carbon paper, Ni/CP, Cu/CP and NiCu/CP electrodes.

Where Q_t was the total consumed electric quantity calculated from the integral discharge current-time curve, and Q_e was theoretically transferred electric quantities based on Reaction (1); C_0 and C_t were initial and final ammonia concentration (mg L^{-1}), respectively; V, F, n were electrolyte volume (10 mL), Faraday constant (96485 C mol^{-1}) and transferred electron number (3) in per mole of Reaction (1).

3. Results and discussion

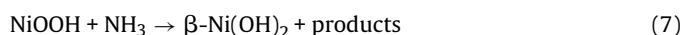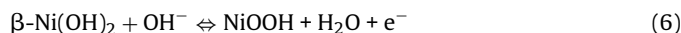### 3.1. Characterization of NiCu/CP electrode

The XRD patterns of pure carbon paper and NiCu/CP were shown in Fig. 1 in order to identify the corresponding crystalline structures of the catalyst. Pure carbon paper had strong peak at 2θ angle of 54°. Typical Ni(111) and Cu$_2$O(111) peaks were observed in the Ni/CP and Cu/CP patterns when sole Ni or Cu element was electrodeposited. However Cu(111) peak was too weak in the Cu/CP patterns to be seen. It indicated that the main deposition product was Cu$_2$O rather than Cu in Cu/CP. When Ni and Cu were co-electrodeposited on carbon paper (NiCu/CP), the Cu$_2$O(111) peak became very weak and Cu(111) and Cu(200) peaks were newly observed at 2θ angles of 43° and 50.3°, respectively. Besides, Ni(111) and Ni(200) peaks were also found at 2θ angles of 44.5° and 52.1° in NiCu/CP patterns. The Ni(111) peak of NiCu/CP was in accordance with that of Ni/CP, and no peak shift was observed, indicating that the NiCu catalyst synthesised on CP by electrochemical co-deposition was bimetal that was composed of two separate metals rather than alloy.

Fig. 2 showed the SEM images of the NiCu/CP electrode. Metal particles were deposited on the carbon fiber uniformly, though some agglomeration of particles was observed. The particle size was about 100 nm. SEM image of NiCu/CP obtained after ammonia electrolysis tests was also conducted and presented no obvious change of NiCu particles on the carbon paper in Fig. 2b, indicating a robust stability of NiCu bimetal. The atom ratio of Ni:Cu was about 5:6 according to EDX measurement (Fig. S1). The SEM images of Ni/CP and Cu/CP were presented in Fig. S2, demonstrating quite different morphology of deposited particles. Ni particles were more densely deposited than NiCu and Cu particles. STEM images of NiCu catalyst together with their elemental distribution are shown in Fig. 2c,d and Fig. S2c. It is evident from Figs. 2d and S2c that the distribution of Ni and Cu are not homogenous, the deposited NiCu particles were found to consist of copper rich and nickel rich regions as well as intermediate compositions.

3.2. Electrochemical properties of the NiCu/CP electrode

Electrochemical measurements were conducted to further characterize the activity and stability of NiCu/CP electrode. Fig. 3a demonstrated the CVs of NiCu/CP electrode in 0.5 M NaOH electrolyte with the presence and absence of 55 mM NH$_3$ respectively. A pair of redox peaks were generated in the CV plots of NiCu/CP in 0.5 M NaOH, which were attributed to the transformation between Ni(II) and Ni(III) species [30,31]. When ammonia was added, a dramatic increase of anodic current density with onset potential about 0.47 V vs. Ag/AgCl could be observed. The anodic current density reached 52 mA cm^{-2} at 0.7 V vs. Ag/AgCl. It demonstrated that NiCu catalyst had obvious activity toward electrooxidation of ammonia.

For comparison, CVs of Ni/CP and Cu/CP were also carried out which are presented in Fig. S3. The black curve in Fig. S3a was the CV curve of Ni/CP in 0.5 M NaOH, which was similar to that of NiCu/CP with a pair of redox peaks. However, there was no obvious change in the red curve of Fig. S3a when ammonia was added, which meant that metal Ni alone did not show catalytic activity in this potential range. This was possibly due to the large overpotential of ammonia electrooxidation on Ni catalyst. In fact Ni catalysts were based on the β-Ni(OH)$_2 \leftrightarrow$NiOOH mechanism in electrocatalytic oxidation reaction [32–34]:

$$\beta\text{-Ni(OH)}_2 + OH^- \Leftrightarrow NiOOH + H_2O + e^- \qquad (6)$$

$$NiOOH + NH_3 \rightarrow \beta\text{-Ni(OH)}_2 + products \qquad (7)$$

NiOOH would be formed from β-Ni(OH)$_2$ via electrochemical Reaction (6) to catalyse the NH$_3$ oxidation and get reduced back to β-Ni(OH)$_2$. According to Reaction (7), NiOOH was the real activated substance. Thus Ni catalyst had to be pre-activated with a transformation routine of Ni $\rightarrow \alpha$-Ni(OH)$_2 \rightarrow \beta$-Ni(OH)$_2 \leftrightarrow (\beta, \gamma)$-NiOOH in alkaline solution [9,10,23]. Moreover, Cu/CP without Ni element was found to have a negligible activity, which demonstrated a low anodic current density (5 mA cm^{-2} at 0.7 V vs. Ag/AgCl) as shown in Fig. S3b. This was because Cu bound the N atom in ammonia too weakly as mentioned in introduction, which could be improved by Ni doping.

Stability is one of the most important parameters to characterize the quality of electrocatalyst. In the present work, the stability of NiCu/CP electrode was examined by chronoamperogram with anode potential fixed at 550 mV vs. Ag/AgCl in 0.5 M NaOH + 55 mM NH$_4$Cl solution. Fig. 3b showed chronoamperogram curves of the NiCu/CP together with Ni/CP and Cu/CP electrodes recorded for nearly 7200 s. For NiCu/CP electrode, the oxidation current density decreased rapidly from the beginning due to the concentration polarization. Then it reached flat with a value of about 8.5 mA cm^{-2}. This result showed that the NiCu/CP electrode was relatively stable in alkaline solutions for ammonia electrooxidation. In comparison, the oxidation current densities of Ni/CP and Cu/CP were very low, about only 0.8 mA cm^{-2} and 0.4 mA cm^{-2}, respectively. The activity of Ni/CP and Cu/CP were too low to be used as anode at this potential, in accordance with the CV results. Higher voltage had to be applied to achieve a desired current density in AEC when using Ni/CP and Cu/CP electrodes, but in that case oxygen evolution reaction might occur and energy efficiency would be very low. This outcome indicated that the NiCu/CP electrode had much higher electrocatalytic activity than that of either Ni/CP or Cu/CP electrode for ammonia oxidation, demonstrating its deep potential to be used as electrocatalyst with enhanced performance. The multi-CVs in 0.5 M NaOH + 55 mM NH$_4$Cl shown in Fig. S4 further testified the stability of NiCu/CP electrode. From the 1st cycle to the 50th cycle, there was an obvious increase of both oxidation and reduction current density. This was attributed to the further activation of NiCu catalyst by possibly formed Ni$_x$Cu$_{1-x}$OOH double oxyhydroxides. Although the copper oxidation/reduction reaction
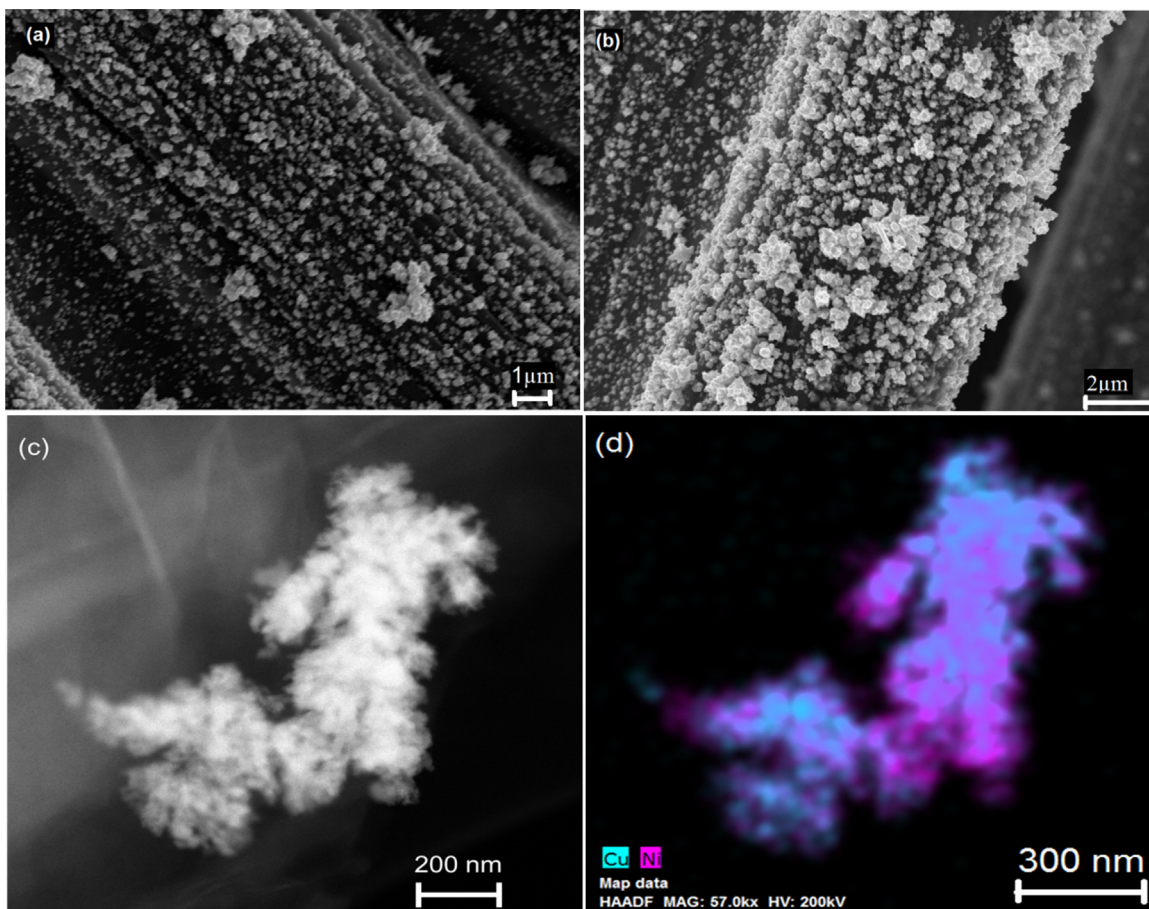
Fig. 2. SEM images of the NiCu/CP electrode (a) before and (b) after ammonia electrolysis tests; (c) STEM images of NiCu catalyst and (d) the Cu, Ni distribution in the NiCu catalyst.
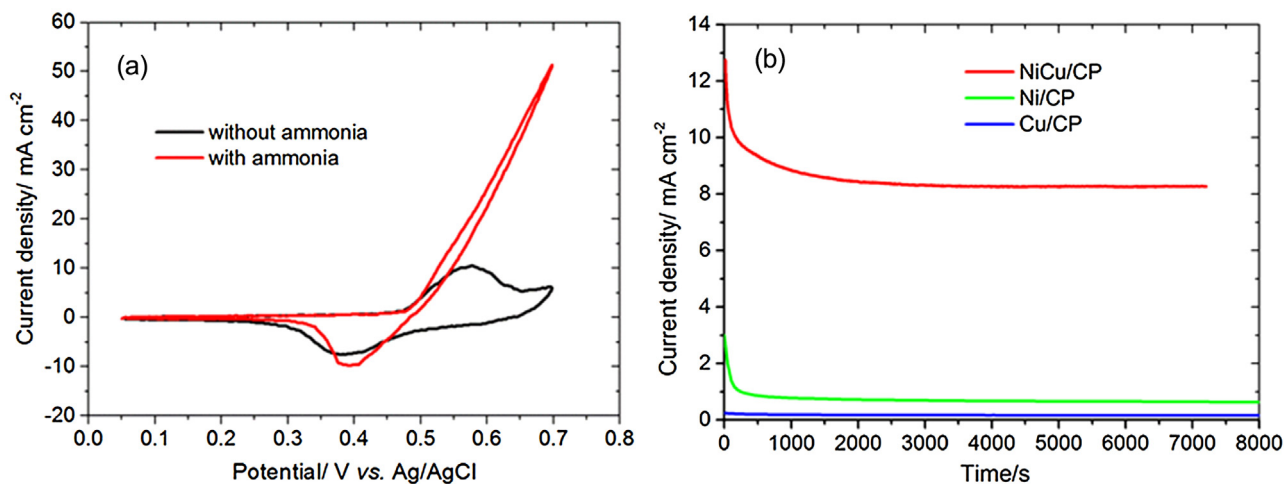

Fig. 3. (a) CVs of NiCu/CP electrode in 0.5 M NaOH with and without 55 mM NH_4Cl; (b) chronoamperogram of Ni/CP, Cu/CP and NiCu/CP electrodes in 0.5 M NaOH with 55 mM NH_4Cl at fixed potential of 0.55 V vs. Ag/AgCl.

might also happen, it was to unable to observe the separated peaks corresponding to these reactions, respectively, implying that Ni, Cu peaks and ammonia oxidation current were partially overlapped. From the 50th cycle to 100th cycle, there was only a slight difference in current density, indicating the strong stability of NiCu/CP in ammonia electrooxidation.

From the XRD patterns of NiCu/CP after electrochemical tests in Fig. S5, new β-Ni(OH)$_2$ phase was observed, indicating that

NiCu bimetallic catalyst might gradually transform to the isomorphous compound as β-Ni(OH)$_2$ under alkaline condition. In order to investigate the surface composition change of NiCu catalysts after electrochemical experiments, XPS was conducted as shown in Fig. 4. Analysis of the Ni 2p and Cu 2p regions was conducted using the work of Biesinger and co-workers as a guide [35,36]. The surface metals of the as-prepared NiCu catalysts before electrochemical tests were oxidized to metal oxides and hydroxide in air
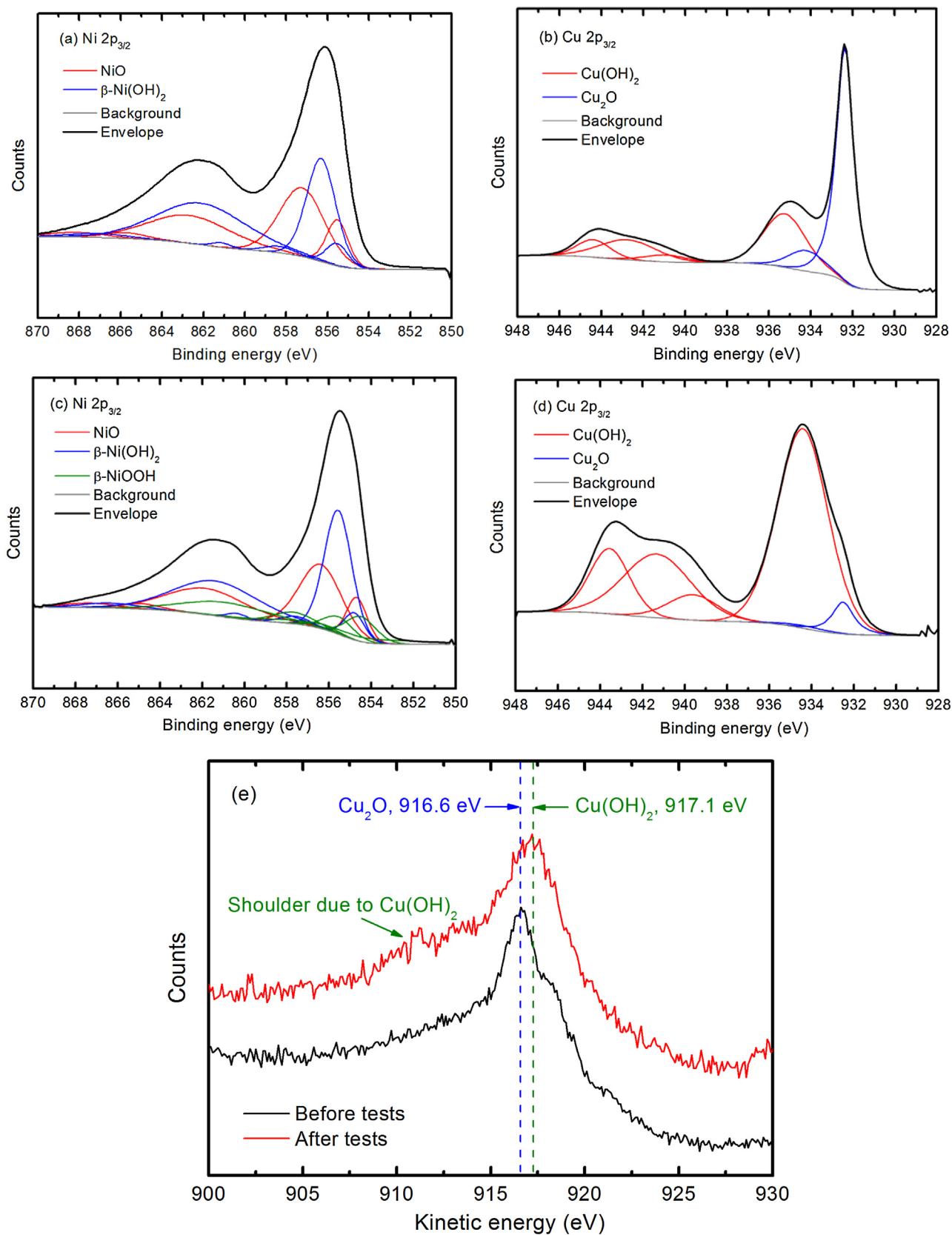
Fig. 4. (a) and (b) XPS spectra of NiCu/CP before tests; (c) and (d) XPS spectra of NiCu/CP after tests; (e) Cu LMM Auger spectra.

according to XPS data in Fig. 4a and Fig. 4b. The oxide and hydroxide phases were not observed in XRD because the signal was too weak to be picked up by X-ray or, they are in amorphous state. Oxygen

was also picked up by high angle annular dark field (HAADF) imagines generated by STEM (Fig. S2) indicating the existing of oxide and/or hydroxide, likely on the surface as the major phase are still

poorly crystallised Ni and Cu as shown in Fig. 1. After electrochemical tests, Ni oxyhydroxides (NiOOH) was newly formed via Reaction (7) as shown in Fig. 4c, and more Ni(OH)$_2$ was observed. Similarly, in Fig. 4d, most of Cu$_2$O was transformed to Cu(OH)$_2$ in alkaline solution after tests. The transformation of Cu(I) to Cu(II) was more clearly proved in Cu LMM Auger spectra in Fig. 4e. The "before" sample had a relatively sharp peak at a kinetic energy of 916.6 eV, whereas the "after" sample seemed more broad and has a peak centred at 917.1 eV. This was due to a shift from a mix of Cu$_2$O and Cu(OH)$_2$ to being predominantly Cu(OH)$_2$. Note that there was also a general shift in the Ni and Cu binding energies (between Fig. 4a–d), with everything related to Ni and Cu moving downward by around 0.8 eV after tests. For example, the β-Ni(OH)$_2$ peak at 855.54 eV before tests shifted to 854.8 eV after tests, and Cu(OH)$_2$ peak at 935.24 eV before tests shifted to 934.41 eV after tests. This interesting phenomenon might be attributed to the formation of NiCu double hydroxide or oxyhydroxides (Ni$_x$Cu$_{1-x}$OOH) in alkaline solution at high potential.

It was reported that Fe incorporating into Ni-based catalysts during the crystallization process would greatly improve the catalysts activity and lower the anode overpotential toward water oxidation reaction [37,38]. This effect might be due to the greatly improvement of conductivities of NiOOH and increase of active sites after Fe dopping [37,38]. In this experiment, Cu incorporating was possible to have a similar effect as Fe to form NiCu double oxyhydroxides and enhance the activity by increasing active sites and conductivity [39]. The electrochemical surface area (ECSA) of NiCu/CP and Ni/CP was measured by scanning CVs in 10 mM K$_3$[Fe(CN)$_6$] with 1 M KCl (Fig. S6). The redox peaks were attributed to the reversible reaction of Fe(CN)$_6{}^{3-}$/Fe(CN)$_6{}^{4-}$. The ECSA was calculated according to Randles–Sevcik equation:

$$i_p = 2.69 \times 10^5 \times n^{1.5}AD^{0.5}Cv^{0.5} \tag{8}$$

where i_p was peak current (A cm^{-2} mg^{-1}); n was the number of electrons involved in the Reaction (1); A was the ECSA; C was the reactant concentration (10^{-5} mol cm^{-3}), D was diffusion coefficient (6.3 × 10^{-6} cm^2 s^{-1}), v was scan rate (0.05 V s^{-1}). The ECSA of NiCu/CP reached 18.4 cm^2 mg^{-1}, which was much larger than that of Ni/CP (8.6 cm^2 mg^{-1}). Higher ECSA might lead to an enhancement of catalytic activity. In addition, the catalyst conductivities could also affect the catalytic activity. In order to test the conductivity, EISs of NiCu/CP and Ni/CP were conducted as shown in Fig. S7. Both NiCu/CP and Ni/CP acquired apparent semicircle in the Nyquist diagrams of both, which should be mainly associated with charge transfer resistance (R$_{ct}$). The diameter of the semicircle of NiCu/CP significantly decreased comparing to that of Ni/CP, indicating much lower charge transfer resistance, i.e. improved conductivity. Accordingly, the high activity of NiCu/CP toward ammonia electrooxidation was due to the synergistic effect of both Ni and Cu. As a result, using NiCu/CP as anode will reduce the electrochemical polarization of oxidation reaction and reduce the energy consumption in AEC.

In order to investigate the influences of electrodeposition conditions, synthesis of NiCu/CP was conducted with different deposition potentials and metal precursor concentrations. NiCu/CP samples were deposited at applied potentials of −1.0 V, −1.15 V, −1.3 V and −1.4 V. The loadings of NiCu on CP were 0.71 mg cm^{-2} (−1.0 V), 0.75 mg cm^{-2} (−1.15 V), 0.79 mg cm^{-2} (−1.3 V) and 0.80 mg cm^{-2} (−1.4 V). The catalytic activities of NiCu/CP prepared at different potentials were tested by CVs in Fig. S8. It was demonstrated that the current density increased when lower potential was applied, but the improvement was not significant. Then the metal precursor concentration was changed to (0.55-X) M Ni^{2+} and X M Cu^{2+} with deposition potential fixed at −1.3 V. The samples of NiCu$_{0.01}$/CP, NiCu$_{0.05}$/CP, NiCu$_{0.125}$/CP, and NiCu$_{0.275}$/CP were obtained from X = 0.01, 0.05, 0.125 and 0.275, respectively. The
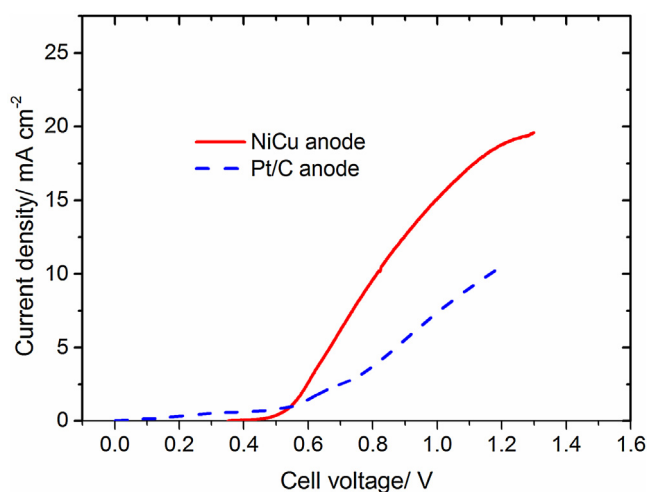

Fig. 5. The LSVs data of NiCu anode (black line) and Pt/C anode (blue line) for AEC in 0.5 M NaOH + 55 mM NH$_4$Cl with a sweep rate of 1 mV s^{-1}. Pt/C cathode was used in both tests. (For interpretation of the references to colour in this figure legend, the reader is referred to the web version of this article.)

loadings of NiCu on CP were 0.79 mg cm^{-2} (X = 0.01), 0.79 mg cm^{-2} (X = 0.05), 1.0 mg cm^{-2} (X = 0.125) and 1.2 mg cm^{-2} (X = 0.275). The catalytic activity of NiCu/CP prepared at different metal precursor concentrations were tested by CVs in Fig. S9. The samples prepared at low Cu^{2+} concentration (X = 0.01 and 0.05) showed slight higher current density. The activities of NiCu/CP electrodes prepared at different conditions were quite close and much higher than that of Ni/CP electrode, indicating wide electrodeposition condition was feasible.

To further investigate the electrooxidation of ammonia on NiCu/CP anode, a two electrode cell with NiCu/CP anode, Pt/C cathode was tested under different conditions. Firstly, the polarization curve of AEC was conducted in 0.5 M NaOH + 55 mM NH$_4$Cl electrolyte using LSV at a sweep rate of 1 mV s^{-1}, as shown in Fig. 5. For comparison, Pt/C anode was also tested in AEC. The applied cell voltage was below the minimal voltage required for water electrolysis, thus the current density was caused by ammonia electrolysis. It was found that the AEC with Pt/C anode demonstrated a very small onset potential due to the low overpotential of ammonia electrooxidation on Pt catalyst, beginning to generate electrolysis current at an applied cell voltage of 0.2 V. The electrolysis current increased with the growth of cell voltage, indicating a growing rate of electrochemical reaction. On the other hand, the AEC with NiCu anode demonstrated an onset potential about 0.3 V larger than that of AEC with Pt/C anode. Despite of this, the electrolysis current of NiCu-AEC increased much faster than that of Pt/C-AEC. The current density of NiCu-AEC reached 16 mA cm^{-2} at an applied cell voltage of 1.0 V, but the current density of Pt/C-AEC reached only about 8 mA cm^{-2} at the same applied voltage. Besides, chronoamperometry analysis demonstrated that the current density of ammonia electrooxidation when using Pt/C had been decreasing from 8.5 mA cm^{-2} to 5 mA cm^{-2} (in Fig. S10), indicating poor stability when compared to NiCu catalyst (in Fig. 3b). This was mainly because that Pt had a potential to be poisoned by the N$_{ads}$ due to the very strong bond between Pt and N atoms, and thus limiting the current density [19,22,40]. In terms of stability and activity for electrooxideation of ammonia, the NiCu bimetal is better than Pt/C.

3.3. Ammonia electrolysis at different pH values

The bulk electrolysis of 500 ppm ammonia at pH = 8, 10, 12 in AEC was conducted during 16 h at constant cell voltage of 1.1 V.
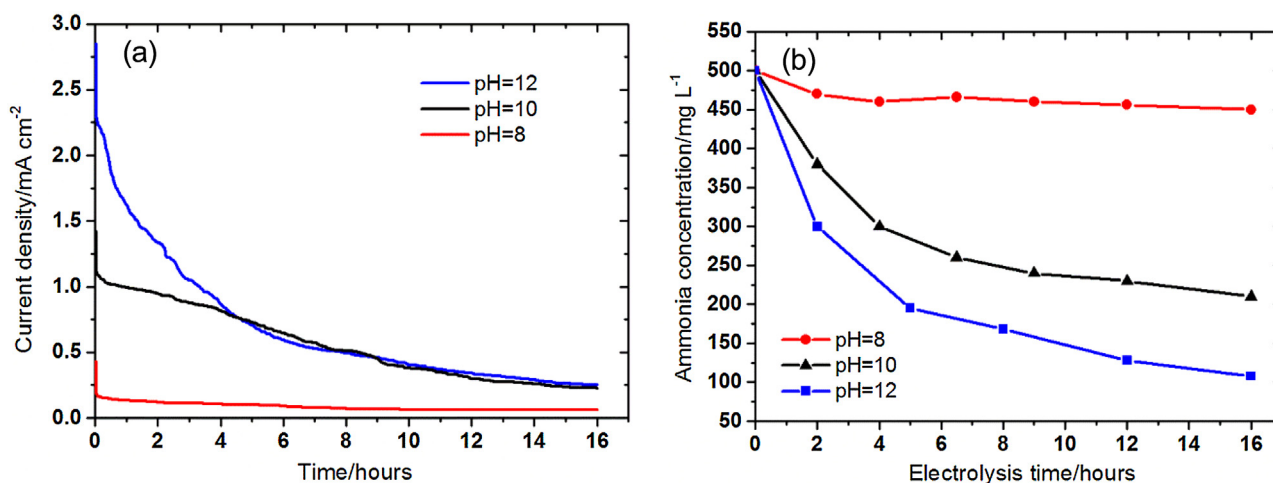
Fig. 6. Bulk electrolysis in AEC with 500 ppm of NH_3 at pH = 8, 10, 12. (a) Records of electrolysis current density and (b) the concentration profile of ammonia during electrolysis. Applied cell voltage was fixed at 1.1 V for all tests.

In a 16-h experiment, current density was recorded and shown in Fig. 6a. All the current densities of the three tests decreased along with electrolysis time, owing to the consumption of ammonia in bulk electrolytes. However, the current responses varied greatly with the pH condition. Higher initial pH value of electrolyte was observed to have a higher current density, leading to faster reaction rate. This highly pH-dependent phenomenon might be caused by the difference of the NiCu catalyst activity. As the activity of NiCu catalyst was based on the formation of $Ni_xCu_{1-x}OOH$ in basic condition, a high pH value would facilitate the transformation of $Ni_xCu_{1-x}(OH)_2$ to $Ni_xCu_{1-x}OOH$ to improve catalytic activity toward ammonia electrooxidation. What's more, the redox potential of ammonia oxidation in Reaction (1), was related to pH value according to Nernst equation: $E = -0.77 + 0.0592(14\text{-pH})$. High pH value would lead to a negative potential (E) and make ammonia electrooxidation reaction easier to proceed in terms of thermodynamics. This was in accordance with the reported work about electrooxidation of ammonia on Ni-based catalyst which shown poor current responses when pH was below 8 [23]. Thus higher pH value could diminish the anode polarization to enhance the current output. The influence of pH on Pt/C anode was similar to NiCu/CP anode as shown in Fig. S11a. On the contrary, higher pH value would lead to a larger polarization on Pt/C cathode as shown in Fig. S11b, but this disadvantage was negligible as cathodic reaction was much easier to reach enough current density with low overpotential when compared to ammonia electrooxidation reaction (anodic reaction).

Ammonia was successfully removed from water during the electrolysis and the concentration change with time was shown in Fig. 6b. Normally there was a positive correlation between AEC current density and ammonia removal rate. The electrolysis at pH = 8 demonstrated a much low current density and ammonia removal efficiency than those at pH = 10 and 12. During a 16-h test, the ammonia concentration with pH = 8 decreased from 500 ppm to ~450 ppm, achieving only 10% efficiency. When the pH rose to 10, the final ammonia concentration reached 210 ppm with a removal efficiency of 58%. For pH = 12, the ammonia concentration reduced quickly in the initial 5 h, and then decreased gradually to 108 ppm at 16 h. However, more NO_3^- tended to generate in higher pH condition. Nitrate ions were detected after ammonia electrolysis, and the results were shown in Table S1. In the test of pH = 12, 14.6% of the degraded NH_3 was recovered as NO_3^-. In comparison, the conversion percent of NH_3 to NO_3^- was only 6.1% and 7.9% when the pH was 8 and 10, respectively.

3.4. Ammonia electrolysis at different cell voltages

The effect of applied cell voltages on ammonia electrolysis was investigated at 1.0 V, 1.2 V and 1.4 V. Fig. 7a demonstrated the current density and ammonia removal efficiency curves with electrolysis time. Higher current densities were achieved when the applied cell voltages increased from 1.0 V to 1.4 V. As the consumption of ammonia, the current densities under all the three cell voltages were observed to decrease gradually. Ammonia removal efficiency was greatly improved when the applied cell voltage increased from 1.0 V to 1.2 V. After 12 h's electrolysis, ammonia removal efficiency reached 51% and 78% when 1.0 V and 1.2 V of cell voltages were applied, respectively. However, there was no obvious improvement on ammonia removal when the applied cell voltage further increased from 1.2 V to 1.4 V, though the current density obtained from 1.4 V shown much higher than current density obtained from 1.2 V. The possible reason was that oxygen evolution reaction might happen and resulted in partially consuming energy in water electrolysis under a cell voltage of 1.4 V. Another reason might be oxidation reaction of carbon paper electrode at high potential:

$$C + 2H_2O \rightarrow CO_2 + 4H^+ + 4e^- \quad E = 0.207\ V vs. SHE \qquad (9)$$
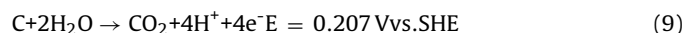
As shown in Fig. 7b, the coulombic efficiency was only 53.1% when the applied cell voltage was 1.4 V, indicating that a portion of generated current was due to the oxygen evolution and carbon oxidation reaction. The ammonia electrolysis at lower cell voltage would lead to a higher coulombic efficiency and was a more energy-efficient way to remove ammonia. The coulombic efficiency reached 92.8%, 81.2% and 74.6%, when the cell voltage was 1.0 V, 1.1 V and 1.2 V, respectively. There was a slight variance of recovery of nitrate from ammonia electrolysis under different cell voltages, as shown in Table S1 (Test 4–6). In addition, the Ni and Cu ions in the final electrolyte were also analysed in order to measure the possible corrosion of NiCu/CP electrode. Results in Table S1 showed that negligible Ni or Cu ions were released to ammonia electrolyte from the NiCu/CP electrode during electrolysis, indicating the stability of NiCu bimetal catalyst had been greatly improved, overcoming the challenge of concomitant release quantity of Ni to the wastewater [23].
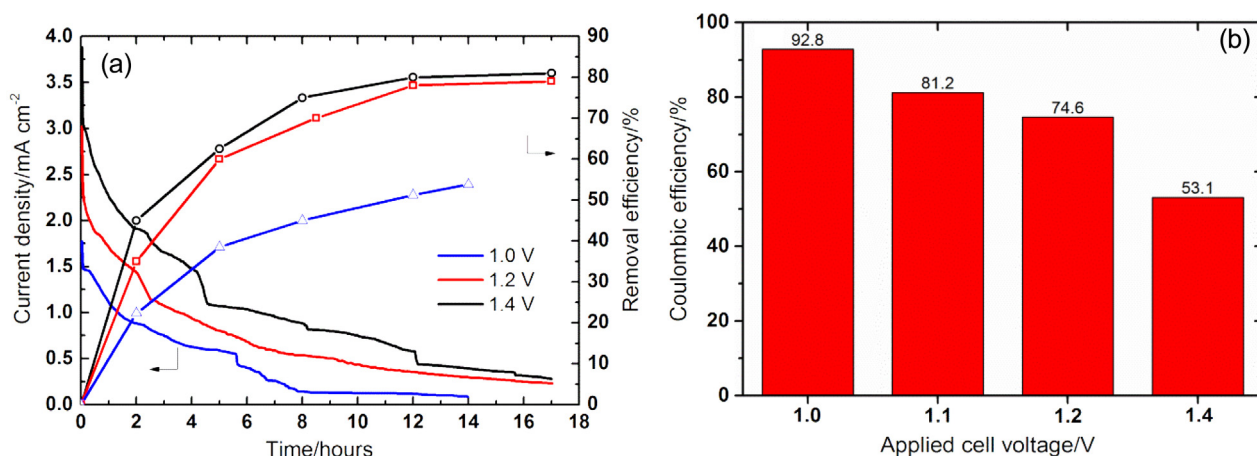
Fig. 7. Bulk electrolysis in AEC with 500 ppm of NH_3 at pH = 12. (a) Records of electrolysis current density and ammonia removal efficiency at different cell voltages of 1.0 V, 1.2 V and 1.4 V, respectively (b) the anodic coulombic efficiency under different cell voltages (the data of 1.1 V was from Fig. 6).
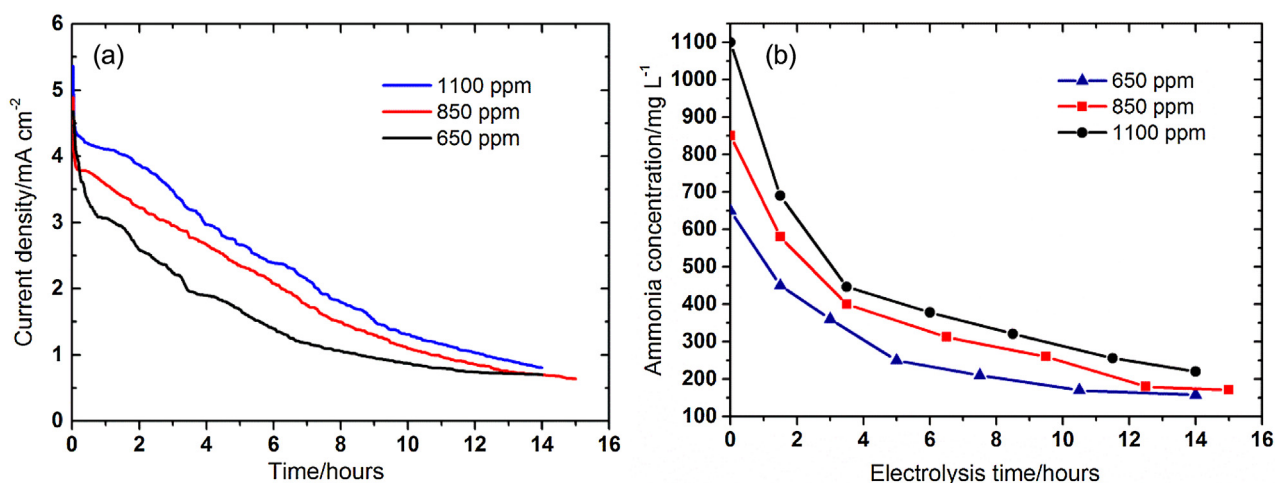

Fig. 8. Bulk electrolysis in AEC with 650, 850, 1100 ppm of NH_3 at pH = 12 and cell voltage of 1.3 V. (a) Records of electrolysis current density and (b) the concentration profile of ammonia during electrolysis.

3.5. Electrolysis with high concentration of ammonia

One of the advantages of electrochemical ammonia treatment is that it can work well at high ammonia concentration conditions. As shown in Fig. 8a, the current density of AEC increased with the ammonia concentration up to a very high value of 1100 ppm. One reason might be that high concentration could improve the mass transfer, as the only mass transfer force in this batch model AEC is the concentration gradient between bulk electrolyte and electrode surface. In addition, there was a competition of adsorbed species such as OH^- on the catalyst surface. More ammonia percent in solution could lead to a higher coverage of catalyst surface by ammonia, thus enhancing ammonia electrooxidation. In comparison, increasing ammonia concentration could not lead to much higher current density of anode reaction when using Pt/C anode (in Fig. S12a). In the aspect of Pt/C cathode reaction, higher ammonia concentration could also enhance cathodic current density due to the improvement of electrolyte conductivity (in Fig. S12b). Fig. 8b demonstrated that ammonia was successfully degraded at high concentration condition. For example, after 14-h experiment, the ammonia concentration was reduced to 220 ppm with initial value of 1100 ppm, reaching a removal efficiency of 80%. Besides, the anodic coulombic efficiency also increased a bit with the higher ammonia concentration, as shown in Fig. S13.

4. Conclusion

Ammonia is regarded as a kind of tough contaminant especially for the high-content wastewater. On the contrary, the AEC equipped NiCu/CP electrode is proved to be suitable for ammonia-rich wastewater due to the improved mass transfer and catalyst surface coverage. NiCu bimetal was prepared by an electrochemical deposition method. XRD, XPS and STEM study indicate the bulk is NiCu bimetal while the surface of the catalyst was oxidised to metal oxide and hydroxide. Experiments show high removal efficiency of around 80% is achieved at both low and high initial concentration (from 500 ppm to 1100 ppm). This AEC could work at low cell voltage to avoid the competitive reaction of water electrolysis and save energy. High coulombic efficiency up to 92.8% is realized at applied cell voltage of 1.0 V. The pH value could largely influence the current density of AEC as well as the formation of nitrate. More NO_3^- ions were formed at higher pH value and higher applied voltage. Therefore low applied voltage is a better choice.

By electrochemical co-deposition of Ni and Cu, the current density is improved by more than 10 times compared to Ni and Cu according to the electrochemical characterization. Higher ECSA was observed for NiCu/CP than that for Ni/CP. In addition, this NiCu bimetallic catalyst demonstrates a strong stability with no poison during the electrolysis which is a big advantage over Pt/C elec-

trode for electrooxidation of ammonia. Therefore it is a promising noble-metal-free catalyst for ammonia electrooxidation. Further improvement and reduction of cost of AEC can possibly be achieved by optimising the cell configuration and the application of non-noble cathode.

Acknowledgements

Appendix A. Supplementary data

Supplementary data associated with this article can be found, in the online version, at http://dx.doi.org/10.1016/j.apcatb.2016.11.003.

References

[1] W.K. Dodds, W.W. Bouska, J.L. Eitzmann, T.J. Pilger, K.L. Pitts, A.J. Riley, J.T. Schloesser, D.J. Thornbrugh, Eutrophication of U.S. freshwaters: analysis of potential economic damages, Environ. Sci. Technol. 43 (2009) 12–19.

[2] S.-L. He, Q. Huang, Y. Zhang, Y.-L. Nie, Evaluation of the performance of different anodes in the electrochemical oxidation of ammonia, Water Air Soil Pollut. 226 (2015) 1–7.

[3] A.Z. Gotvajn, T. Tišler, J. Zagorc-Končan, Comparison of different treatment strategies for industrial landfill leachate, J. Hazard. Mater. 162 (2009) 1446–1456.

[4] T.A. Kurniawan, W.-h. Lo, G.Y.S. Chan, Physico-chemical treatments for removal of recalcitrant contaminants from landfill leachate, J. Hazard. Mater. 129 (2006) 80–100.

[5] T. Khin, A.P. Annachhatre, Novel microbial nitrogen removal processes, Biotechnol. Adv. 22 (2004) 519–532.

[6] G. Zhan, L. Zhang, D. Li, W. Su, Y. Tao, J. Qian, Autotrophic nitrogen removal from ammonium at low applied voltage in a single-compartment microbial electrolysis cell, Bioresour. Technol. 116 (2012) 271–277.

[7] H. Qin, B. Molitor, J.T. Brazil, Recovery of nitrogen and water from landfill leachate by a microbial electrolysis cell–forward osmosis system, Bioresour. Technol. 200 (2016) 485–492.

[8] Y. Vanlangendonck, D. Corbisier, A. Van Lierde, Influence of operating conditions on the ammonia electro-oxidation rate in wastewaters from power plants (ELONITA™ technique), Water Res. 39 (2005) 3028–3034.

[9] A. Allagui, S. Sarfraz, S. Ntais, F. Al momani, E.A. Baranova, Electrochemical behavior of ammonia on Ni98Pd2 nano-structured catalyst, Int. J. Hydrogen Energy 39 (2014) 41–48.

[10] A. Allagui, S. Sarfraz, E.A. Baranova, Ni$_x$Pd$_{1-x}$ (x = 0.98, 0.93, and 0.58) nanostructured catalysts for ammonia electrooxidation in alkaline media, Electrochim. Acta 110 (2013) 253–259.

[11] Z. Ni, J. Liu, Y. Wu, B. Liu, C. Zhao, Y. Deng, W. Hu, C. Zhong, Fabrication of platinum submonolayer electrodes and their high electrocatalytic activities for ammonia oxidation, Electrochim. Acta 177 (2015) 30–35.

[12] L. Li, Y. Liu, Ammonia removal in electrochemical oxidation: mechanism and pseudo-kinetics, J. Hazard. Mater. 161 (2009) 1010–1016.

[13] L. Candido, J.A.C.P. Gomes, Evaluation of anode materials for the electro-oxidation of ammonia and ammonium ions, Mater. Chem. Phys. 129 (2011) 1146–1151.

[14] H. Zöllig, E. Morgenroth, K.M. Udert, Inhibition of direct electrolytic ammonia oxidation due to a change in local pH, Electrochim. Acta 165 (2015) 348–355.

[15] A. Estejab, D.A. Daramola, G.G. Botte, Mathematical model of a parallel plate ammonia electrolyzer for combined wastewater remediation and hydrogen production, Water Res. 77 (2015) 133–145.

[16] R. Lan, J.T.S. Irvine, S.W. Tao, Ammonia and related chemicals as potential indirect hydrogen storage materials, Int. J. Hydrogen Energy 37 (2012) 1482–1494.

[17] R. Lan, S.W. Tao, Direct ammonia alkaline anion-exchange membrane fuel cells, Electrochem. Solid State Lett. 13 (2010) B83–B86.

[18] R. Lan, S.W. Tao, Ammonia carbonate fuel cells based on a mixed NH$_4^+$/H$^+$ ion conducting electrolyte, ECS Electrochem. Lett. 2 (2013) F37–F40.

[19] C. Zhong, W.B. Hu, Y.F. Cheng, Recent advances in electrocatalysts for electro-oxidation of ammonia, J. Mater. Chem. A 1 (2013) 3216–3238.

[20] L.A. Diaz, G.G. Botte, Mathematical modeling of ammonia electrooxidation kinetics in a Polycrystalline Pt rotating disk electrode, Electrochim. Acta 179 (2015) 519–528.

[21] L.A. Diaz, G.G. Botte, Hydrodynamic analysis and simulation of a flow cell ammonia electrolyzer, Electrochim. Acta 179 (2015) 529–537.

[22] J.A. Herron, P. Ferrin, M. Mavrikakis, Electrocatalytic oxidation of ammonia on transition-Metal surfaces: a first-Principles study, J. Phys. Chem. C 119 (2015) 14692–14701.

[23] A. Kapałka, A. Cally, S. Neodo, C. Comninellis, M. Wächter, K.M. Udert, Electrochemical behavior of ammonia at Ni/Ni(OH)2 electrode, Electrochem. Commun. 12 (2010) 18–21.

[24] K. Yao, Y.F. Cheng, Investigation of the electrocatalytic activity of nickel for ammonia oxidation, Mater. Chem. Phys. 108 (2008) 247–250.

[25] X. Zhao, M. Fuji, T. Shirai, H. Watanabe, M. Takahashi, Electrocatalytic activity of the conductive alumina/NCN composite electrode by electro-depositing NiCu particles for methanol oxidation, J. Am. Ceram. Soc. 94 (2011) 1167–1172.

[26] M. Motlak, N.A.M. Barakat, A.G. El-Deen, A.M. Hamza, M. Obaid, O.B. Yang, M.S. Akhtar, K.A. Khalil, NiCu bimetallic nanoparticle-decorated graphene as novel and cost-effective counter electrode for dye-sensitized solar cells and electrocatalyst for methanol oxidation, Appl. Catal. A: Gen. 501 (2015) 41–47.

[27] S.H. Ahn, H.-Y. Park, I. Choi, S.J. Yoo, S.J. Hwang, H.-J. Kim, E. Cho, C.W. Yoon, H. Park, H. Son, J.M. Hernandez, S.W. Nam, T.-H. Lim, S.-K. Kim, J.H. Jang, Electrochemically fabricated NiCu alloy catalysts for hydrogen production in alkaline water electrolysis, Int. J. Hydrogen Energy 38 (2013) 13493–13501.

[28] S. De, J. Zhang, R. Luque, N. Yan, Ni-based bimetallic heterogeneous catalysts for energy and environmental applications, Energy Environ. Sci. 9 (2016), http://dx.doi.org/10.1039/C1036EE02002J.

[29] D. Saranya, Electrodeposition of Ni–Cu alloys from a protic ionic liquid medium-voltammetric and surface morphologic studies, J. Electroanal. Chem. 734 (2014) 70–78.

[30] W. Xu, H. Zhang, G. Li, Z. Wu, Nickel-cobalt bimetallic anode catalysts for direct urea fuel cell, Sci. Rep. 4 (2014) 5863.

[31] W. Yan, D. Wang, G.G. Botte, Nickel and cobalt bimetallic hydroxide catalysts for urea electro-oxidation, Electrochim. Acta 61 (2012) 25–30.

[32] W. Huang, J. Zheng, Z. Li, New oscillatory electrocatalytic oxidation of amino compounds on a nanoporous film electrode of electrodeposited nickel hydroxide nanoflakes, J. Phys. Chem. C 111 (2007) 16902–16908.

[33] X. Cui, W. Guo, M. Zhou, Y. Yang, Y. Li, P. Xiao, Y. Zhang, X. Zhang, Promoting effect of Co in NimCon (m + n = 4) bimetallic electrocatalysts for methanol oxidation reaction, ACS Appl. Mater. Interfaces 7 (2015) 493–503.

[34] J. Nai, Z. Chen, H. Li, F. Li, Y. Bai, L. Li, L. Guo, Structure-dependent electrocatalysis of Ni(OH)2 hourglass-like nanostructures towards L-histidine, Chem. Eur. J. 19 (2013) 501–508.

[35] M.C. Biesinger, L.W.M. Lau, A.R. Gerson, R.S.C. Smart, Resolving surface chemical states in XPS analysis of first row transition metals, oxides and hydroxides: sc, Ti, V, Cu and Zn, Appl. Surf. Sci. 257 (2010) 887–898.

[36] M.C. Biesinger, B.P. Payne, A.P. Grosvenor, L.W.M. Lau, A.R. Gerson, R.S. Smart, Resolving surface chemical states in XPS analysis of first row transition metals, oxides and hydroxides: cr, Mn, Fe, Co and Ni, Appl. Surf. Sci. 257 (2011) 2717–2730.

[37] S. Klaus, Y. Cai, M.W. Louie, L. Trotochaud, A.T. Bell, Effects of Fe electrolyte impurities on Ni(OH)2/NiOOH structure and oxygen evolution activity, J. Phys. Chem. C 119 (2015) 7243–7254.

[38] S.L. Trotochaud, J.K. Young, Nickel–Iron oxyhydroxide oxygen-evolution electrocatalysts: the role of intentional and incidental iron incorporation, J. Am. Chem. Soc. 136 (2014) 6744–6753.

[39] O. Diaz-Morales, I. Ledezma-Yanez, M.T.M. Koper, F. Calle-Vallejo, Guidelines for the rational design of Ni-Based double hydroxide electrocatalysts for the oxygen evolution reaction, ACS Catal. 5 (2015) 5380–5387.

[40] M.H.M.T. Assumpção, R.M. Piasentin, P. Hammer, R.F.B. De Souza, G.S. Buzzo, M.C. Santos, E.V. Spinacé, A.O. Neto, J.C.M. Silva, Oxidation of ammonia using PtRh/C electrocatalysts: fuel cell and electrochemical evaluation, Appl. Catal. B: Environ. 174–175 (2015) 136–144.